Fast three-step phase-shifting algorithm

Peisen S. Huang and Song Zhang

We propose a new three-step phase-shifting algorithm, which is much faster than the traditional three-step algorithm. We achieve the speed advantage by using a simple intensity ratio function to replace the arctangent function in the traditional algorithm. The phase error caused by this new algorithm is compensated for by use of a lookup table. Our experimental results show that both the new algorithm and the traditional algorithm generate similar results, but the new algorithm is 3.4 times faster. By implementing this new algorithm in a high-resolution, real-time three-dimensional shape measurement system, we were able to achieve a measurement speed of 40 frames per second at a resolution of 532 × 500 pixels, all with an ordinary personal computer.

OCIS codes: 120.0120, 120.2650, 100.5070.

1. Introduction

Phase wrapping in the phase-shifting method is the process of determining the phase values of the fringe patterns in the range of 0 to 2π.[1] Phase unwrapping, on the other hand, is the process of removing the 2π discontinuity to generate a smooth phase map of the object.[2] Many algorithms have been developed to increase the processing speed of phase unwrapping.[3–5] However, few discussions have been focused on increasing the speed of phase-wrapping algorithm. Traditional phase-wrapping algorithms involve the calculation of an arctangent function, which is too slow in the case when real-time processing is required.[6] Wan and Lin proposed a phase reduction algorithm that uses the intensity of a fringe image to approximate the phase.[7] The resulting phase error is eliminated by averaging two reductions with $\pi/2$ difference in phase. Even though its calculation of phase based on intensity is fast, this algorithm requires finding the fringe centers and normalizing the fringe patterns before phase calculation, which slows down the processing. The averaging method does eliminate most part of the error, but not all. The residual error may still be significant depending on applications. Besides, when used for applications other than interferometric testing of optics, the potential existence of texture patterns on the object surface can cause errors in finding fringe centers, thus making the algorithm less reliable.

In recent years, we have been developing a high-resolution, real-time three-dimensional (3D) shape measurement system based on the phase-shifting method.[8,9] As the phase-shifting algorithm for the system, the three-step algorithm has been our choice because it requires the minimum number of fringe images among all the existing algorithms. Less number of images means faster image capture as well as processing, which translates into higher measurement speed. However, our experiments show that even with the three-step algorithm, the image processing speed is still not fast enough for real-time 3D shape reconstruction when an ordinary personal computer is used.[6] The bottleneck lies in the calculation of phase, which involves a computationally time-consuming arctangent function. To solve this problem, we propose a new three-step algorithm, which replaces the calculation of the arctangent function with a simple intensity ratio calculation and therefore is much faster than the traditional algorithm. The phase error caused by this replacement is compensated for by use of a lookup table (LUT). Our experimental results show that both the new algorithm and the traditional algorithm generate similar results, but the new algorithm is 3.4 times faster. The adoption of this new algorithm enabled us to successfully build a high-resolution, real-time 3D shape measurement system that captures, reconstructs, and displays the 3D shape of the measured object at a speed of 40 frames per

P. S. Huang is with the Department of Mechanical Engineering, State University of New York (SUNY) at Stony Brook, Stony Brook, New York 11794-2300. S. Zhang (szhang@fas.harvard.edu) is with the Department of Mathematics, Harvard University, Cambridge, Massachusetts 02138.

Received 1 November 2005; revised 6 March 2006; accepted 7 March 2006; posted 13 March 2006 (Doc. ID 65703).

0003-6935/06/215086-06$15.00/0

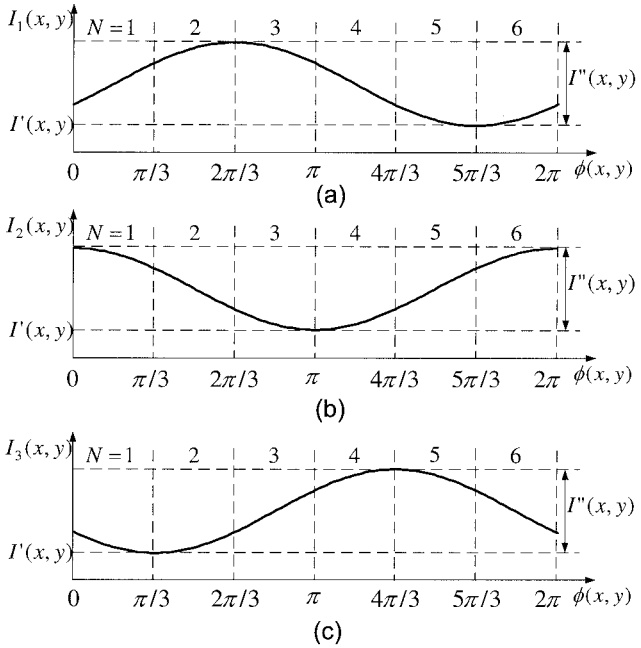

Fig. 1. Cross sections of the three phase-shifted sinusoidal fringe patterns. (a) $I_1(\alpha = -120°)$. (b) $I_2(\alpha = 0°)$. (c) $I_3(\alpha = 120°)$.

second (fps) and a resolution of 532×500 pixels, all with an ordinary personal computer.[10]

Section 2 describes the principle of the proposed algorithm. Section 3 discusses the error of the algorithm and proposes an error compensation method. Section 4 presents some experimental results. Finally, Section 5 summarizes the work.

2. Principle

Among the various phase-shifting algorithms available,[1] the three-step algorithm requires the minimum number of frames and is the simplest to use. The following equations describe the intensity values of the three measured fringe patterns:

$$I_1(x, y) = I'(x, y) + I''(x, y)\cos[\phi(x, y) - \alpha], \quad (1)$$

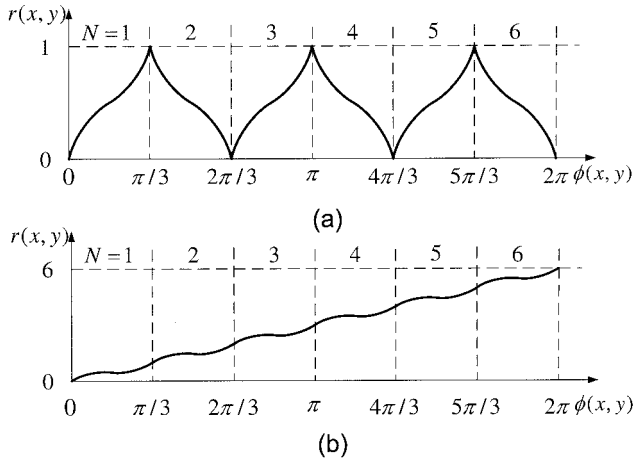

Fig. 2. Cross sections of the intensity ratio image and the phase image. (a) Intensity ratio. (b) Phase.

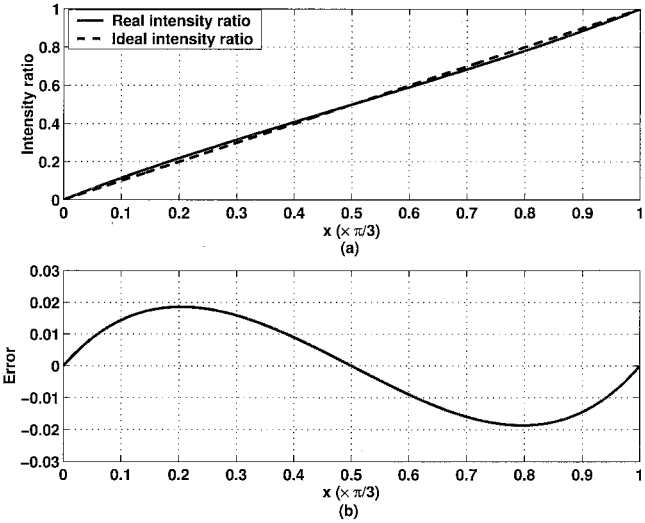

Fig. 3. (Color online) Nonlinearity error caused by the use of the fast three-step algorithm. (a) Intensity ratio in the region $N = 1$. (b) Nonlinearity error.

$$I_2(x, y) = I'(x, y) + I''(x, y)\cos[\phi(x, y)], \quad (2)$$

$$I_3(x, y) = I'(x, y) + I''(x, y)\cos[\phi(x, y) + \alpha], \quad (3)$$

where $I'(x, y)$ is the average intensity, $I''(x, y)$ is the intensity modulation, $\phi(x, y)$ is the phase, and α is the phase step size. Even though α can be any value, the two commonly used ones are $\alpha = 90°$ and $\alpha = 120°$. The fast phase-shifting algorithm described in this paper applies only to the case of $\alpha = 120°$. For $\alpha = 120°$, solving Eqs. (1) to (3) for the phase yields

$$\phi(x, y) = \arctan\left(\sqrt{3}\,\frac{I_1 - I_3}{2I_2 - I_1 - I_3}\right). \quad (4)$$

Since computers are not that good at computing the arctangent function, the traditional approach of calculating the phase using Eq. (4) directly is relatively slow.

We encountered this problem in our effort to develop a real-time 3D shape measurement system based on fringe projection and phase shifting.[8,11] As a solution, we proposed a novel phase-shifting method, namely, the trapezoidal phase-shifting method, that used trapezoidal fringe patterns instead of the traditional sinusoidal ones.[6] By calculating an intensity ratio using a simple function, instead of phase using the arctangent function, we were able to increase the calculation speed by 4.6 times, which made the real-time reconstruction of 3D shapes possible. However, the use of trapezoidal fringe patterns brought some error due to image defocus, even though the error is small, especially when compared to the traditional intensity-ratio based methods.[12–15] In the course of trying to deal with this error, we discovered that if we apply the algorithm developed for the trapezoidal method to sinusoidal patterns, considering the sinusoidal patterns as the defocused trapezoidal patterns, and then com-

pensate for the small error due to defocus, we could preserve the calculation speed of the trapezoidal method while achieving the same accuracy of the traditional sinusoidal phase-shifting algorithm. The principle is described in the following paragraphs.

Figure 1 shows the cross sections of the three phase-shifted sinusoidal patterns with a phase step size of 120°. We divide the period evenly into six regions ($N = 1, 2, \ldots, 6$), each covers an angular range of 60°. In each region, the three curves do not cross. Therefore, we can denote the three intensity values to be $I_{\min}(x, y)$, $I_{\text{med}}(x, y)$, and $I_{\max}(x, y)$, which are the minimum, median, and maximum intensity values, respectively. From these three intensity values, we can calculate the so-called intensity ratio $r(x, y)$ as follows:

$$r(x, y) = \frac{I_{\text{med}}(x, y) - I_{\min}(x, y)}{I_{\max}(x, y) - I_{\min}(x, y)}, \tag{5}$$

which has a value between 0 and 1, as shown in Fig. 2(a). The phase can then be calculated by the following equation:

$$\phi'(x, y) = \frac{\pi}{3}\left[2 \times \text{round}\left(\frac{N-1}{2}\right) + (-1)^{N-1} r(x, y)\right], \tag{6}$$

whose value ranges from 0 to 2π, as shown in Fig. 2(b). As we can see from the figure, the phase calculation is not accurate, but with a small error. In Section 3, we analyze this error and discuss how this error can be compensated for.

If multiple fringes are used, the phase calculated by Eq. (6) will result in a sawtoothlike shape, just as in the traditional phase-shifting algorithm. In this case, the traditional phase-unwrapping algorithm has to be used to obtain the continuous phase map.[2]

3. Error Analysis and Compensation

The fast three-step algorithm has the advantage of fast processing speed over the traditional three-step algorithm. However, this method makes the linear phase value $\phi(x, y)$ nonlinear, as shown in Fig. 2(b), which produces error. In this section, we discuss the error caused by applying the fast three-step algorithm for sinusoidal patterns first and then propose an error compensation method.

From Fig. 2(b), we see that the error is periodical and the pitch is $\pi/3$. Therefore, we only need to analyze the error in one period, say, $\phi(x, y) \in [0, \pi/3)$. In this period, $I_{\max}(x, y) = I_2(x, y)$, $I_{\text{med}}(x, y) = I_1(x, y)$, and $I_{\min}(x, y) = I_3(x, y)$. By substituting Eqs. (1) to (3) into Eq. (5), we obtain

$$r(\phi) = \frac{I_1 - I_3}{I_2 - I_3} = \frac{1}{2} + \frac{\sqrt{3}}{2}\tan\left(\phi - \frac{\pi}{6}\right). \tag{7}$$

The right-hand side of this equation can be considered as the sum of a linear and a nonlinear terms. That is,

$$r(\phi) = \frac{\phi}{\pi/3} + \Delta r(\phi), \tag{8}$$

where the first term represents the linear relationship between $r(x, y)$ and $\phi(x, y)$ and the second term $\Delta r(x, y)$ is the nonlinearity error, which can be calculated as follows:

$$\Delta r(\phi) = r(\phi) - \frac{\phi}{\pi/3} = \frac{1}{2} + \frac{\sqrt{3}}{2}\tan\left(\phi - \frac{\pi}{6}\right) - \frac{\phi}{\pi/3}. \tag{9}$$

Figure 3(a) shows the plots of both the ideal linear ratio and the real nonlinear ratio. Their difference, which is similar to a sine wave in shape, is shown in Fig. 3(b). By taking the derivative of $\Delta r(x, y)$ with respect to $\phi(x, y)$ and setting it to zero, we can determine that when

$$\phi = \frac{\pi}{6} \pm \cos^{-1}\left(\sqrt{\sqrt{3}\pi/6}\right), \tag{10}$$

the ratio error reaches its maximum and minimum values, respectively, as

$$\Delta r(\phi)_{\max} = \Delta r(\phi)\big|_{\phi=\phi_1} = 0.0186, \tag{11}$$

$$\Delta r(\phi)_{\min} = \Delta r(\phi)\big|_{\phi=\phi_2} = -0.0186. \tag{12}$$

Therefore, the maximum ratio error is $\Delta r(\phi)_{\max} - \Delta r(\phi)_{\min} = 0.037$. Even though this error is relatively small, it needs to be compensated for when accurate measurement is required.

Since the ratio error is a systematic error, it can be compensated for by using an LUT method. In this research, an 8-bit camera is used. Therefore the LUT is constructed with 256 elements, which represent the error values determined by $\Delta r(\phi)$. If a higher-bit-depth camera is used, the size of the LUT should be increased accordingly. Because of the periodical nature of the error, this same LUT can be applied to all six regions. Finally, it should be noted that the phase error can be found by simply multiplying the intensity ratio error by $\pi/3$.

4. Experiments

To verify the effectiveness of the proposed algorithm experimentally, we used a projector to project sinusoidal fringe patterns onto the object and an 8-bit black-and-white (B/W) CCD camera with 532×500 pixels to capture the three phase-shifted fringe images.[9] First, we used a flat board as the target object. The captured three fringe images are shown in Fig. 4(a)–4(c). For comparison, we applied both the traditional algorithm and the newly proposed algorithm to the same fringe images. Figures 5(a), 5(b), and 5(c) show the intensity ratio errors of the traditional three-step

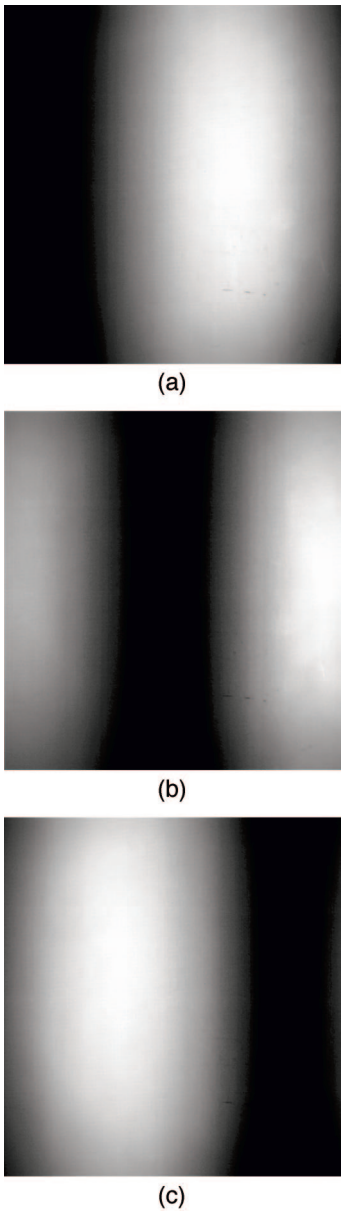

Fig. 4. Fringe images of a flat board captured by an 8-bit B/W CCD camera. (a) Fringe image $I_1(\alpha = -120°)$. (b) Fringe image $I_2(\alpha = 0°)$. (c) Fringe image $I_3(\alpha = 120°)$.

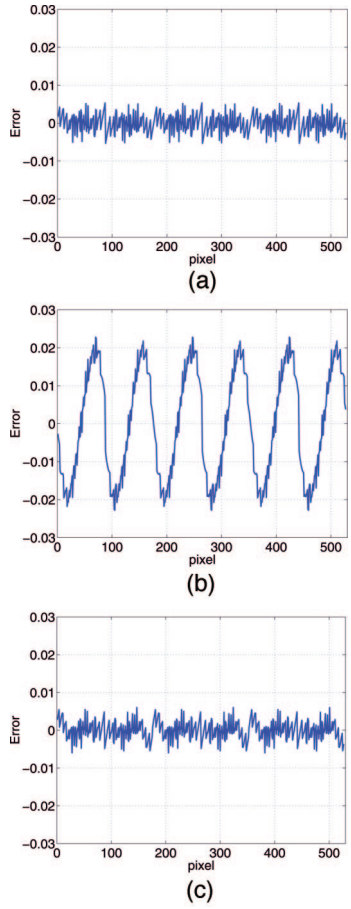

Fig. 5. (Color online) Intensity ratio error ($\times\pi/3$ for phase error). (a) With the traditional three-step algorithm. (b) With the fast three-step algorithm before error compensation. (c) With the fast three-step algorithm after error compensation.

algorithm, the fast three-step algorithm before error compensation, and the fast three-step algorithm after error compensation, respectively. From Fig. 5(b), we see that the intensity ratio error (phase error) of the fast three-step algorithm before error compensation is approximately 0.04 (0.042 radians), which is only slightly larger than the theoretical value of 0.037 (0.039 radians) due to the existence of noise. After error compensation, this error, which is shown in Fig. 5(c), is significantly reduced and is comparable to that of the traditional three-step algorithm as shown in Fig. 5(a).

Next, we measured an object with more complex surface geometry, a Lincoln head sculpture. The fringe images are shown in Figs. 6(a)–6(c) and the two-dimensional (2D) photo of the object is shown in Fig. 6(d). The reconstructed 3D shapes based on the traditional and the proposed three-step algorithms are shown in Figs. 6(e) and 6(f), respectively. The phase difference was found to be less than RMS 0.0002 radians.

In our experiment, we used an ordinary personal computer (Pentium 4, 2.8 GHz) for image processing. The traditional three-step algorithm took 20.8 ms, while the proposed new algorithm took only 6.1 ms, which was 3.4 times less. The improvement in processing speed is significant. To demonstrate its usefulness, we implemented this new algorithm in our real-time 3D data acquisition system[9] and successfully realized real-time 3D shape acquisition, reconstruction, and display at 40 fps with a image resolution of 532 × 500. In this system, a PC workstation with dual CPUs (2.8 GHz) and a parallel processing program were used to accomplish the task. Figure 7 shows the experimental setup for the real-time 3D system. The captured 3D shape is projected in real time onto a white board on the side of the object. Figure 8 shows the experiment of using our real-time system to capture human facial expressions. The image on the left is the face of a human

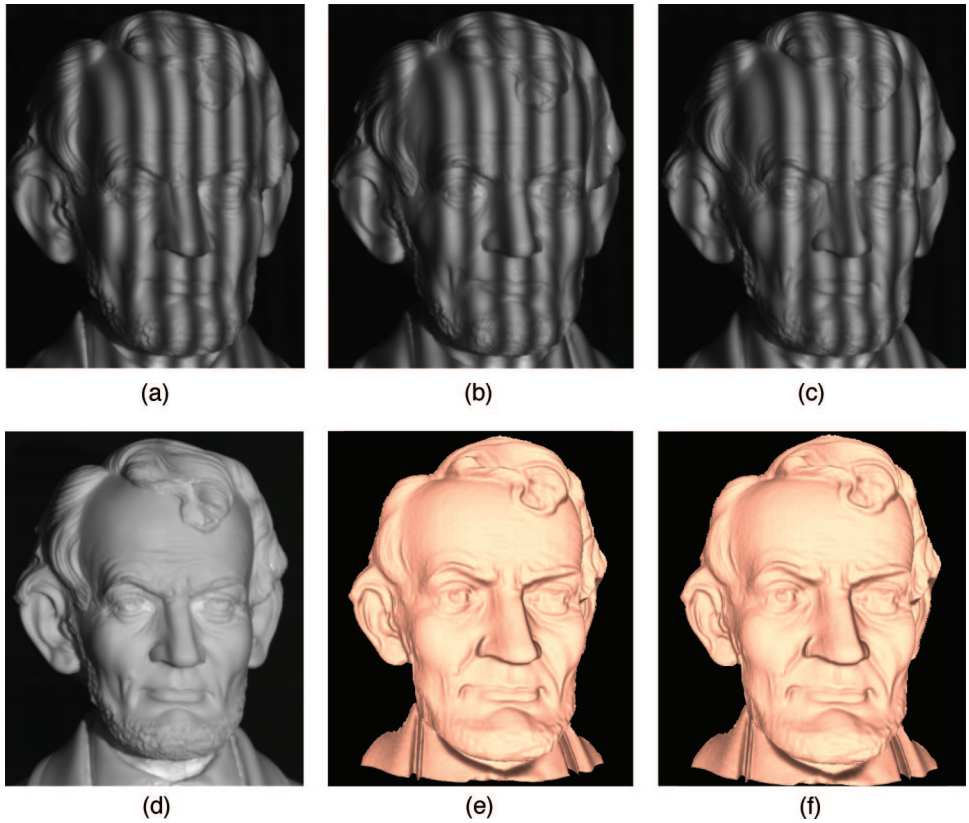

Fig. 6. (Color online) Measurement results of a Lincoln head sculpture. (a) Fringe image $I_1(\alpha = -120°)$. (b) Fringe image $I_2(\alpha = 0°)$. (c) Fringe image $I_3(\alpha = 120°)$. (d) 2D photo. (e) 3D shape by the traditional three-step algorithm. (f) 3D shape by the fast three-step algorithm.

subject, while the image on the right is the 3D shape of the face generated by our system in real time.

5. Conclusions

In this paper, we proposed a fast three-step phase-shifting algorithm based on intensity ratio calculation and LUT error compensation for real-time 3D shape measurement. This algorithm originated from the previously proposed trapezoidal phase-shifting method, which was aimed at improving the processing speed of the fringe images. In this research, we found that the same algorithm developed for the trapezoidal fringe patterns could be used to process sinusoidal fringe images with a small error, which could be easily eliminated by using an LUT method. This finding resulted in a new three-step phase-shifting algorithm that is 3.4 times faster than and just as accurate as the traditional three-step algorithm. Experimental results demonstrated the effectiveness of the proposed algorithm. We have successfully imple-

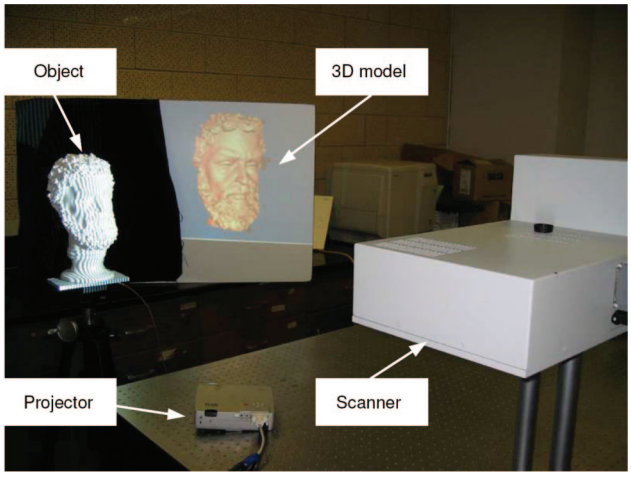

Fig. 7. (Color online) Experimental setup for real-time 3D shape acquisition, reconstruction, and display.

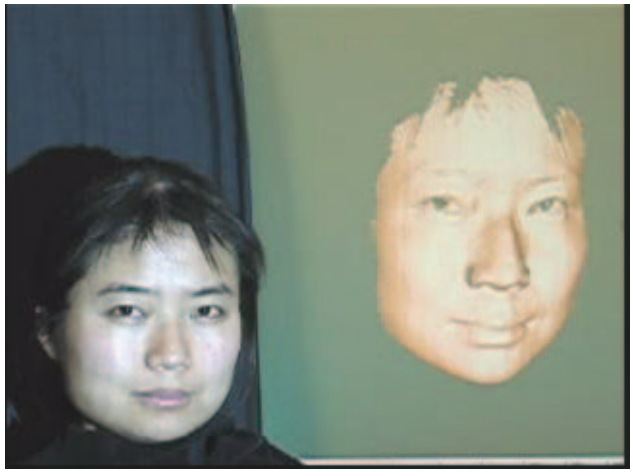

Fig. 8. (Color online) Real-time measurement of human facial expressions.

mented this algorithm in our real-time 3D shape measurement system, which resulted in a frame rate of 40 fps and a resolution of 532 × 500 points.

This work was supported by the National Science Foundation under grant CMS-9900337 and the National Institute of Health under grant RR13995.

References

1. D. Malacara, ed., *Optical Shop Testing* (Wiley, 1992).
2. D. C. Ghiglia and M. D. Pritt, *Two-Dimensional Phase Unwrapping: Theory, Algorithms, and Software* (Wiley, 1998).
3. M. A. Herráez, D. R. Burton, M. J. Lalor, and M. A. Gdeisat, "Fast two-dimensional phase-unwrapping algorithm based on sorting by reliability following a noncontinuous path," Appl. Opt. **41,** 7437–7444 (2002).
4. M. A. Herráez, M. A. Gdeisat, D. R. Burton, and M. J. Lalor, "Robust, fast, and effective two-dimensional automatic phase unwrapping algorithm based on image decomposition," Appl. Opt. **41,** 7445–7455 (2002).
5. A. Asundi and W. Zhou, "Fast phase-unwrapping algorithm based on a gray-scale mask and flood fill," Appl. Opt. **37,** 5416–5420 (1998).
6. P. Huang, S. Zhang, and F.-P. Chiang, "Trapezoidal phase-shifting method for 3-D shape Measurement," in *Two- and Three-Dimensional Vision Systems for Inspection, Control, and Metrology II,* K. G. Harding, ed., Proc. SPIE **5606,** 142–152 (2004).
7. D.-S. Wan and D.-T. Lin, "Ronchi test and a new phase reduction algorithm," Appl. Opt. **29,** 3255–3265 (1990).
8. P. S. Huang, C. Zhang, and F. P. Chiang, "High-speed 3-D shape measurement based on digital fringe projection," Opt. Eng. **42,** 163–168 (2003).
9. S. Zhang and P. Huang, "High-resolution, real-time 3-D shape acquisition," presented at the IEEE Computer Vision and Pattern Recognition Workshop (CVPRW'04), Washington, D.C., 27 June–2 July 2004.
10. S. Zhang, "High-resolution, real-time 3D shape measurement," Ph.D. thesis (State University of New York at Stony Brook, 2005).
11. C. Zhang, P. S. Huang, and F.-P. Chiang, "Microscopic phase-shifting profilometry based on digital micromirror device technology," Appl. Opt. **41,** 5896–5904 (2002).
12. B. Carrihill and R. Hummel, "Experiments with the intensity ratio depth sensor," Comput. Vis. Graph. Image Process. **32,** 337–358 (1985).
13. T. Miyasaka, K. Kuroda, M. Hirose, and K. Araki, "Reconstruction of realistic 3D surface model and 3D animation from range images obtained by real time 3D measurement system," in *Proceedings of the International Conference on Pattern Recognition 2000* (IEEE, 2000), pp. 594–598.
14. T. Miyasaka, K. Kuroda, M. Hirose, and K. Araki, "High speed 3-D measurement system using incoherent light source for human performance analysis," in *XIXth Congress of the International Society for Photogrammetry and Remote Sensing,* K. J. B. M. Molenaar, ed. (ISPRS, 2000), pp. 16–23.
15. G. Chazan and N. Kiryati, "Pyramidal intensity-ratio depth sensor," Tech. Rep. 121 (Israel Institute of Technology, 1995).